

# Improved sampling strategies for ensemble-based optimization

K.R. Ramaswamy<sup>1,2</sup>, O. Leeuwenburgh<sup>2</sup>, R.M. Fonseca<sup>2</sup>  
M.M. Siraj<sup>1</sup>, P.M.J. Van den Hof<sup>1</sup>

<sup>1</sup> Eindhoven University of Technology, <sup>2</sup> TNO

December 21, 2017

## Abstract

We are concerned with the efficiency of stochastic gradient estimation methods for solving large-scale nonlinear optimization problems in the presence of uncertainty. These techniques aim to estimate an approximate gradient from a limited number of random control vector samples and the corresponding objective function values. Ensemble methods usually employ Gaussian sampling to generate the control samples. It is known from optimal design theory that the quality of sample-based approximations is affected by the distribution of the samples. We investigate if optimal sampling designs lead to improved gradient estimates, and subsequently to improved performance of the optimization process. We apply six different sampling strategies to optimization of a high-dimensional analytical benchmark problem, and, in a second example, to optimization of oil reservoir management strategies with and without geological uncertainty. The effectiveness of the sampling strategies is analyzed based on the quality of the estimated gradient, the final objective function value, the rate of convergence and the robustness of the gradient estimate. We find that  $UE(s^2)$  sampling strategies motivated by optimal design theory for supersaturated cases outperform all alternative approaches, including quasi-random sampling and LHS designs. We also introduce two new strategies that outperform the  $UE(s^2)$  designs previously suggested in the literature.

## Introduction

A continuous increase over recent decades in computing power, accompanied by improvements in numerical algorithms, has led to increasing use of simulation models to obtain optimal operating strategies for complex systems. Simulation of these models may be very computationally demanding and will therefore require highly efficient numerical optimization workflows. One domain in which computational demands are continuously challenging the efficiency of optimization workflows is the management of subsurface (e.g.

oil) reservoirs. This problem can be characterized by large-scale multiphase and compositional flow models, high-dimensional control spaces, and by large geological, economical and operational uncertainty. The presence of significant uncertainty, even after years of data gathering, motivates the optimization of the expected value of the objective function, an approach that is sometimes referred to as robust optimization (Van Essen et al., 2009).

Controls may include the number of wells to be drilled (10-100's), their locations and trajectories, the drilling order, the well type (injector or producer) as well as operational controls such as well rates or pressures over a period of several years. The total number of variables to be optimized can easily be in the order of 1000's. Gradient-based methods have been shown to be the most efficient techniques to find optimal solutions for these complex problems (Brouwer and Jansen (2004), Sarma et al. (2008), Jansen et al. (2008) and Van den Hof et al. (2009)). In many practical cases of interest the types of controls (e.g. integer or categorical) and lack of access to the numeric model code prevents use of efficient gradient estimation by means of the adjoint method.

In such scenarios approximate gradient methods that require a limited number of test simulations with perturbed controls as input have been proven to be quite useful. An advantage of this approach is that it treats the model as a black box, and therefore offers great flexibility in terms of the type of controls that can be considered. The main challenge associated with this approach is to ensure that the approximate gradients are accurate enough to enable sufficient increases in the objective function at reasonable computational cost. Since test simulations can be performed in parallel (assuming the availability of a parallel computing facility), this challenge translates into choosing the control perturbation set (ensemble) in such a way that the gradients can be estimated with minimal error.

Various methods exist for gradient approximation. Deterministic methods include finite differences and the simplex gradient (Custodio and Vicente, 2007), both of which are computationally unattractive for large numbers of controls since they require as many perturbation tests runs as there are controls. Stochastic approaches based on a limited number of random perturbations include Simultaneous Perturbation Stochastic Approximation (SPSA) (Spall, 1992) and Stochastic Noise Reaction (SNR) (Okano and Koda, 2003), both of which are based on averaging, and Ensemble Optimization (EnOpt) (Chen, 2008) and a modified version coined Stochastic Simplex Approximate Gradient (StoSAG) (Fonseca et al. (2014); Fonseca et al. (2016)), which are both based on least-squares linear regression. Do and Reynolds (2013) discussed the relationship between some of these methods in a deterministic context.

The sampling strategy (distribution) used to generate the ensemble of controls is extremely important but has received little attention in the literature. In Fonseca et al. (2015a) the impact of ensemble size on the quality of the ensemble gradient was investigated for the Rosenbrock function and for an oil reservoir model. It was also shown that the perturbation size (the standard deviation of a multivariate Gaussian distribution) has a significant impact on the gradient quality. A method to adaptively adjust the perturbation size through Covariance Matrix Adaptation (CMA) was suggested by Fonseca et al. (2015b) and was called CMA-EnOpt. Sarma and Chen (2014) investigated the impact

73 of a quasi-random sampling method (Sobol sampling, Niederreiter (1988)) that avoids  
 74 clustering of samples on SNR gradient estimates. They found Sobol sampling to lead to a  
 75 faster rate of convergence relative to Gaussian sampling when applied to a deterministic  
 76 reservoir optimization problem. The performance of Sobol sampling strategies in a robust  
 77 optimization context was not investigated.

78 Considering that the number of controls ( $N$ ) for the problems of interest will nor-  
 79 mally be much larger than the feasible number of test simulations ( $M$ ) we will be dealing  
 80 here exclusively with the underdetermined (supersaturated) case. Specifically we will ad-  
 81 dress the question which sampling strategy for the supersaturated case leads to optimal  
 82 performance of eapproximate gradient estimation methods within large-scale nonlinear  
 83 optimization problems under uncertainty. We investigate three categories of sampling:  
 84 quasi-random (low-discrepancy) sequences, stratified sampling, and sampling designs moti-  
 85 vated by optimality criteria. All sampling methods are applied in combination with the  
 86 StoSAG gradient estimation method.

87 In the remainder of this paper, we first provide a brief review of ensemble optimization  
 88 for both deterministic and robust cases in Section 2, followed by a discussion of the various  
 89 sampling strategies used in this paper (Sobol sampling, Latin Hypercube Sampling (LHS),  
 90  $UE(s^2)$  - optimal supersaturated design) and the motivation for considering them in  
 91 Section 3. Here we also introduce two new variants of  $UE(s^2)$  - optimal supersaturated  
 92 design. Finally in Section 4 the sampling strategies are applied in conjunction with the  
 93 StoSAG method first to the extended Rosenbrock optimization test function (Dixon and  
 94 Mills, 1994) and subsequently to a synthetic 3D reservoir model of realistic complexity  
 95 (for both deterministic and robust cases) followed by a detailed analysis.

## 96 Ensemble-based gradient estimation

97 Chen (2008) proposed a stochastic gradient estimation method for use within an ensemble-  
 98 based optimization workflow referred to as EnOpt. Modified versions for determin-  
 99 istic and robust optimization problems were suggested by Do and Reynolds (2013)  
 100 and Fonseca et al. (2014) respectively. A discussion of approximation errors associ-  
 101 ated with the original and modified versions was presented by Fonseca et al. (2016).  
 102 They also coined the acronym Stochastic Simplex Approximate Gradient (StoSAG) for  
 103 the modified version to highlight the relationship with the Simplex gradient (Kelly,  
 104 1999). While the Simplex gradient estimation method is a full-rank deterministic  
 105 method, the StoSAG method is a low-rank stochastic method based on random per-  
 106 turbations. With low-rank we mean that the estimation typically involves fewer equa-  
 107 tions than unknowns. Consider the objective function  $J(\mathbf{u}, \mathbf{m})$  of the control vector  
 108  $\mathbf{u} = [u_1, \dots, u_N]^T$  and of model parameter vector  $\mathbf{m}$ . Given an ensemble of control  
 109 perturbation vectors  $\mathbf{U} = [\delta\mathbf{u}^1 \dots \delta\mathbf{u}^M]^T$  and corresponding objective function values  
 110 anomalies  $\mathbf{j} = [J(\mathbf{u} + \delta\mathbf{u}^1, \mathbf{m}) - J(\mathbf{u}, \mathbf{m}), \dots, J(\mathbf{u} + \delta\mathbf{u}^M, \mathbf{m}) - J(\mathbf{u}, \mathbf{m})]^T$  a first-order  
 111 Taylor expansion of  $J$  around  $\mathbf{u}$  leads to the linear system of equations

$$U\mathbf{g} \approx \mathbf{j} \quad , \quad (1)$$

112 from which we wish to estimate the gradient  $\mathbf{g}$ . Here it was assumed that the objective  
 113 function can be evaluated using a single model with known parameters  $\mathbf{m}$ . If the model  
 114 is considered uncertain, one may choose to define an expected objective function  $\bar{J}(\mathbf{u}) =$   
 115  $\frac{1}{M} \sum_{i=1}^M J(\mathbf{u}, \mathbf{m}^i)$  instead. It can be shown (Fonseca et al., 2016) that in this case the  
 116 expected gradient  $\bar{\mathbf{g}}$  can be estimated by solving a single system like Eq. (1) with  $\mathbf{j}$   
 117 replaced by  $\tilde{\mathbf{j}} = [J(\mathbf{u} + \delta\mathbf{u}^1, \mathbf{m}^1) - J(\mathbf{u}, \mathbf{m}^1), \dots, J(\mathbf{u} + \delta\mathbf{u}^M, \mathbf{m}^M) - J(\mathbf{u}, \mathbf{m}^M)]^\top$ ,

$$U\bar{\mathbf{g}} \approx \tilde{\mathbf{j}} \quad . \quad (2)$$

118 In the following we will refer to the optimization problem corresponding to Eq. (1) as  
 119 deterministic, and to the case corresponding to Eq. (2) as robust optimization. The normal  
 120 equations can be formulated by pre-multiplying with  $\mathbf{U}^\top$ , leading for the deterministic  
 121 case to

$$\mathbf{U}^\top \mathbf{U} \mathbf{g} \approx \mathbf{U}^\top \mathbf{j} \quad . \quad (3)$$

122 The matrix  $\mathbf{U}^\top \mathbf{U}$  has dimension  $N \times N$ . Since the number of perturbations  $M$  that we  
 123 can afford to evaluate (i.e. the number of equations) is typically less than  $N$ , the number  
 124 of controls, the  $N \times N$  matrix  $\mathbf{U}^\top \mathbf{U}$  is rank deficient and its inverse does not exist. A  
 125 unique solution is normally obtained by imposing a minimum norm constraint and can  
 126 be computed from the generalized pseudoinverse as

$$\hat{\mathbf{g}} = \mathbf{U}^\dagger \mathbf{j} = (\mathbf{U}^\top \mathbf{U})^\dagger \mathbf{U}^\top \mathbf{j} \quad . \quad (4)$$

It was shown in Stordal et al. (2016) that if  $\{\mathbf{z}^i\}_{i=1}^M$  with  $\mathbf{z}^i = \mathbf{u} + \delta\mathbf{u}^i = \mathbf{u}^i$  is an i.i.d.  
 sample from the multivariate Gaussian density  $\mathcal{N}(\mathbf{u}, \mathbf{C}_u)$ , the ensemble gradient (4) has  
 the following convergence property (in the almost sure sense) for  $M \rightarrow \infty$

$$\hat{\mathbf{g}} = (\mathbf{U}^\top \mathbf{U})^\dagger \mathbf{U}^\top \mathbf{j} = \left( \frac{1}{M} \mathbf{U}^\top \mathbf{U} \right)^\dagger \frac{1}{M} \sum_{i=1}^M (\mathbf{z}^i - \mathbf{u})(J(\mathbf{z}^i) - J(\mathbf{u})) \quad (5)$$

$$\xrightarrow{a.s.} \mathbf{C}_u^{-1} \int (J(\mathbf{z}) - J(\mathbf{u})) (\mathbf{z} - \mathbf{u}) \mathcal{N}(\mathbf{z}|\mathbf{u}, \mathbf{C}_u) d\mathbf{z} \quad (6)$$

$$= \int J(\mathbf{z}) \nabla_{\mathbf{u}} \mathcal{N}(\mathbf{z}|\mathbf{u}, \mathbf{C}_u) d\mathbf{z} \quad (7)$$

127 In other words, the ensemble gradient (4) is a Monte Carlo (i.e. random sampling-based)  
 128 approximation of a probability-weighted integral of the function values  $J(\mathbf{u}^i)$  over all  
 129 possible values of  $\mathbf{u}^i$ . The convergence properties of such an approximation will depend  
 130 strongly on the chosen sampling strategy (Caffisch, 1998).

### 131 Sampling strategies

132 In the context of estimation, the matrix  $\mathbf{U}$  is known as the design matrix and the matrix  
 133  $\mathbf{S} = (\mathbf{U}^\top \mathbf{U})$  as the information matrix. The choice for a set of samples is that for  
 134 a particular design and can be motivated by the desired statistical properties of the

135 solution of Eq. (4). These properties generally depend on properties of the matrix  $\mathbf{S}$   
136 or, equivalently, of its inverse, known as the dispersion matrix, and lead to a number of  
137 optimality criteria which will be discussed later in this section. If  $M \geq N$  and the rank of  
138  $\mathbf{U}$  is equal to or greater than  $N$ , the solution Eq. (4) is the best linear unbiased estimator  
139 (BLUE) and has variance proportional to  $\mathbf{S}^{-1}$ . In the case that  $M < N$ , which is most  
140 relevant here, the solution (4) is the minimum bias estimator. If  $M = N$  and the elements  
141  $S_{ij} = 0$  for all  $i \neq j$ , the design is called orthogonal.

#### 142 Random sampling

143 Random sampling (or Monte-Carlo sampling) is the conventional approach to generate  
144 control perturbations for ensemble-base gradient estimation. A generic approach to gen-  
145 erating samples is to obtain random combinations of basis vectors that are obtained by  
146 factorization of a perturbation covariance matrix  $\mathbf{C}_u$ , for example by Cholesky decompo-  
147 sition,  $\mathbf{C}_u = \mathbf{L}^T \mathbf{L}$ , such that  $\delta \mathbf{u}^i = \mathbf{L} r^i$ , where  $r^i$  is a number from a pseudo-random  
148 sequence as can be generated by random number generators available with any computer  
149 code. The standard distribution used for ensemble gradient estimation is the Gaussian  
150 distribution, i.e.  $r \propto \mathcal{N}(0, \mathbf{C}_u)$ . If perturbations are uncorrelated,  $\mathbf{C}_u = \sigma^2 \mathbf{I}_N$ . In some  
151 cases, for example when the controls represent long time series discretized in short in-  
152 tervals (typical for the oil reservoir well control problem), a regularized solution may be  
153 obtained by imposing time correlation between subsequent controls. In this case  $\mathbf{C}_u$  will  
154 be a block-diagonal matrix.

#### 155 Quasi Monte-Carlo sampling

156 We have already seen that the ensemble gradient estimation is equivalent with a Monte-  
157 Carlo integration (also known as quadrature). The Quasi Monte-Carlo (QMC) method  
158 (Morokoff and Caffisch, 1995) is an alternative to the Monte-Carlo (MC) method for  
159 calculating this approximation using quasi-random (deterministic) sequences with higher  
160 convergence rate than obtained with (pseudo) random sequences. The improved con-  
161 vergence originates from the uniformity of the quasi-random sampling distribution. The  
162 uniformity is quantified by the discrepancy which measures the relative density of sam-  
163 ples in each sub-volume of the half-open unit cube. Low-discrepancy sequences have  
164 good uniformity properties (Caffisch, 1998) Examples of low-discrepancy quasi-random  
165 sequences are the Sobol, Halton and Fraure sequences. More detailed discussion of quasi-  
166 random sequences and their properties is provided by e.g. Niederreiter (1978). Given  
167 their low-discrepancy properties, which avoid clustering of samples in sub-volumes, they  
168 are good candidates for generating space-filling designs (Caffisch, 1998). In this work we  
169 will present results obtained with the Sobol sequence which tends to produce lower corre-  
170 lations in high dimensions than Halton sampling (Morokoff and Caffisch (1995); Cavazzuti  
171 (2013)). Successful application of Sobol sequences in problems of dimension 300 have  
172 been reported in the literature (Paskov and Traub, 1995).

### 173 Stratified sampling

174 A number of approaches that directly address the error variance of the Monte Carlo  
 175 estimate are discussed in Caffisch (1998). Stratification is a variance reduction technique  
 176 that, like low-discrepancy sampling, attempts to avoid the clustering of samples. Latin  
 177 Hypercube Sampling (LHS) (McKay et al., 1979) is perhaps the best known stratified  
 178 sampling method that is suitable for higher dimensions and settings where  $M < N$  (Owen,  
 179 2013). LHS divides the input (design) space equally into  $M$  strata (sub-domains), an  
 180 arrangement known as Latin squares, and places a sample randomly in each stratum.  
 181 McKay et al. (1979) and Owen (1997) provide theoretical reasoning to show that LHS  
 182 can be much better than MC sampling and it cannot be much worse. However, Diego et al.  
 183 (2016) report that LHS methods may produce clustering of samples in high dimensions.

184 Figure 1 shows examples of Gaussian and Uniform (pseudo) random, quasi-random  
 185 (Sobol), and stratified (LHS) sample distributions for a simple 2-control example and 100  
 186 samples, that is  $N = 2$  and  $M = 100$ . While this different from the  $M < N$  case of  
 187 interest, the figure serves as a simple illustration of the motivation for considering sample  
 188 distributions other than Gaussian. In order to enable comparison of the sample spread  
 189 the standard deviation was normalized to 1 in both directions for all four distributions.  
 190 Gaussian sampling produces relatively dense sampling around the center, as expected.  
 191 LHS appears to produce sampling distributions that are very similar to uniform sampling,  
 192 at least for the case  $M > N$ , with some clustering and under-sampled intervals. Sobol  
 193 sampling can be seen to produce a uniform space filling sample distribution.

### 194 Optimal supersaturated designs

195 The theory of Design of Experiments (DOE) distinguishes saturated ( $M = N$ ) and non-  
 196 saturated ( $M > N$ ) designs. It furthermore defines a number of design criteria and  
 197 techniques to obtain designs that satisfy these criteria. Here we are interested primar-  
 198 ily in designs for the supersaturated case based on the  $E(s^2)$  criterion which defines an  
 199 approximate orthogonality measure (Booth and Cox, 1962). An extension, the so-called  
 200  $UE(s^2)$ -optimal supersaturated designs (Jones and Majumdar, 2014) add an effective  
 201 design optimality criterion (D-optimality).

202 For a supersaturated design, the information matrix  $\mathbf{S}$  becomes rank deficient and  
 203 hence its inverse does not exist. A natural approach in this case is to find a design that  
 204 is nearly orthogonal, that is, the design in which the absolute values of the off-diagonal  
 205 elements of the matrix  $\mathbf{S}$  are small in some sense. Booth and Cox (1962) suggested two  
 206 alternative approaches to obtain near-orthogonal designs. The first is to choose a design  
 207 with minimum  $\max_{i \neq j} |s_{ij}|$  and among all such designs to choose one with the fewest  $s_{ij}$   
 208 that achieve this maximum. The second approach is to choose a design in which the sum  
 209 of the squares of the off-diagonal elements is minimum, that is, a design that minimizes

$$E(s^2) = \frac{2}{(N-1)(N-2)} \sum_{i < j} s_{ij}^2 \quad , \quad (8)$$



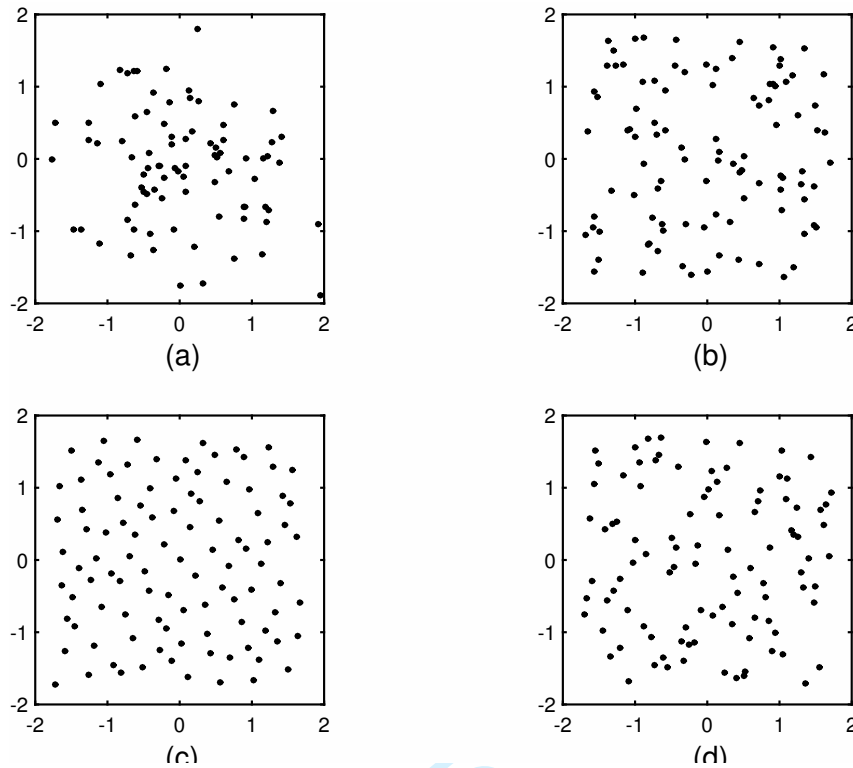


**Figure 1: Example of 2D sample distributions with standard deviation 1. (a) Gaussian, (b) Uniform, (c) Sobol, (d) LHS.**

210 which is called the  $E(s^2)$  criterion. A design is  $E(s^2)$ -optimal if it satisfies the following  
 211 conditions:

- 212 1.  $s_{1j} = 0 \forall j = 2, \dots, N$
- 213 2. among all those designs that satisfy 1, the design should minimize  $E(s^2)$  given in  
 214 Eq. (8).

215 This design is called an  $E(s^2)$ -optimal, or near-orthogonal, supersaturated design. There  
 216 are various methods for construction of  $E(s^2)$ -optimal supersaturated designs (Gilmour,  
 217 2006), but we will consider only the methods using Hadamard matrices (Lin (1993); Wu  
 218 (1993)).

219 Optimal designs are experimental designs for which the solution of the estimator satis-  
 220 fies particular statistical optimality criteria. Generally, these statistical criteria are formu-  
 221 lated in terms of the (generalized) variance of the solution, for example, minimum trace  
 222 of the covariance of  $\hat{\mathbf{g}}$  (A-optimality), minimum maximum eigenvalue of the covariance  
 223 of  $\hat{\mathbf{g}}$  (E-optimality), or minimum product of non-zero eigenvalues of the covariance of  $\hat{\mathbf{g}}$   
 224 (D-optimality) (de Aguiar et al., 1995). The  $E(s^2)$  design can be made more theoretically  
 225 strong and efficient by adding such traditional design optimality criteria.  $UE(s^2)$ -optimal  
 226 design are designs for the supersaturated case that are near-orthogonal but exchange  
 227 the first constraint above for D-optimality.  $UE(s^2)$ -optimal supersaturated designs could

228 therefore be described as producing minimum bias minimum variance estimates. For details  
 229 about algorithms for their construction from Hadamard matrices we refer to Jones  
 230 and Majumdar (2014). A brief summary of the general procedure and variants is provided  
 231 here.

232 A Hadamard matrix  $\mathbf{H} \in \mathbb{R}^{N \times N}$  is a square matrix whose columns are orthogonal to  
 233 each other and for which holds that  $\mathbf{H}\mathbf{H}^T = \mathbf{H}^T\mathbf{H} = N\mathbf{I}_N$  where  $\mathbf{I}_N$  is the identity  
 234 matrix of size  $N \times N$ . It consists of elements  $\pm 1$  and it is generally available for order  
 235  $N$  equal to 1, 2 and multiples of 4. Procedures for constructing a  $UE(s^2)$ -optimal design  
 236 matrix  $\mathbf{U} \in \mathbb{R}^{M \times N}$  with  $M < N$  from Hadamard matrices are discussed by Jones and  
 237 Majumdar (2014), who also review modern methods to construct Hadamard matrices of  
 238 the required orders. Four situations can be distinguished based on the remainder of  $N$   
 239 when divided by 4 that are referred to as  $T_0$ ,  $T_1$ ,  $T_2$  and  $T_3$ . In the following,  $N = a(\text{mod}$   
 240  $4)$  means  $a$  is the remainder when  $N$  is divided by 4.

- 241 1.  $T_0$ : If  $N = 0(\text{mod } 4)$ ,  $2 \leq M \leq N-1$ . Start with a normalized Hadamard matrix of  
 242 order  $N$ ,  $\mathbf{H}_N$ .  $\mathbf{U}$  can be formed by selection of any  $M$  rows of  $\mathbf{H}_N$ .
- 243 2.  $T_1$ : If  $N = 1(\text{mod } 4)$ ,  $2 \leq M \leq N-1$ . Start with a normalized Hadamard matrix of  
 244 order  $N-1$ ,  $\mathbf{H}_{N-1}$ . Let  $\mathbf{V}$  be a  $M \times (N-1)$  matrix formed by any  $M$  rows of  $\mathbf{H}_{N-1}$   
 245 and let  $\phi$  be an (arbitrary)  $M \times 1$  vector with entries 1 or -1.  $\mathbf{U} = (\mathbf{V}, \phi)$ .
- 246 3.  $T_2$ : If  $N = 2(\text{mod } 4)$ ,  $2 \leq M \leq N-2$ .
  - 247 i.  $M$  is even,  $M = 2p$ . Start with a normalized Hadamard matrix of order  $N-2$ ,  
 248  $\mathbf{H}_{N-2}$ . Let  $\mathbf{U}^*$  be the  $M \times (N-2)$  matrix formed by any  $M$  rows of  $\mathbf{H}_{N-2}$ . Let  
 249  $\mathbf{X}_1$  be a  $M \times 2$  matrix with each of the first  $p$  rows either (1,1) or (-1,-1) and each  
 250 of the last  $p$  rows either (1,-1) or (-1,1). Then  $\mathbf{U} = (\mathbf{U}^*, \mathbf{X}_1)$ .
  - 251 ii.  $M$  is odd,  $M = 2p+1$ . Start with a normalized Hadamard matrix of order  $N-2$ ,  
 252  $\mathbf{H}_{N-2}$ . Let  $\mathbf{U}^*$  be the  $M \times (N-2)$  matrix formed by any  $M$  rows of  $\mathbf{H}_{N-2}$ . Let  
 253  $\mathbf{X}_2$  be a  $M \times 2$  matrix with each of the first  $p$  rows either (1,1) or (-1,-1) and each  
 254 of the last  $p+1$  rows either (1,-1) or (-1,1). Then  $\mathbf{U} = (\mathbf{U}^*, \mathbf{X}_2)$ .
- 255 4.  $T_3$ : If  $N = 3(\text{mod } 4)$ ,  $2 \leq M \leq N-1$ . Start with a normalized Hadamard matrix of  
 256 order  $N+1$ ,  $\mathbf{H}_{N+1}$ . Let  $\mathbf{U}^*$  be the  $M \times (N+1)$  matrix formed by any  $M$  rows of  
 257  $\mathbf{H}_{N+1}$ . Suppose the last column of  $\mathbf{U}^*$  is denoted by  $\phi$  and  $\mathbf{U}^* = (\mathbf{U}, \phi)$ . Thus  $\mathbf{U}$   
 258 can be obtained.

259 Given that there is some freedom in constructing the Hadamard matrices, we will  
 260 consider three variants for constructing  $\mathbf{U}$  denoted as M1, M2 and M3 as explained  
 261 below.

- 262 1. M1: This is the approach suggested by Jones and Majumdar (2014). In the con-  
 263 struction of  $UE(s^2)$  optimal designs of Types  $T_0$  to  $T_3$ , it is suggested to take  $M$   
 264 arbitrary rows of a Hadamard matrix. By choosing the rows randomly in each iter-  
 265 ation of the optimization, variation in the samples can be achieved without loss of  
 266  $UE(s^2)$  optimality. Thus the method becomes stochastic.



- 267 2. M2: This approach is similar to Type M1 except that the row of the Hadamard  
 268 matrix containing only values of +1 is always picked. When Type M1 is used, this  
 269 row may not always be picked. Experiments presented below showed that in those  
 270 instances, gradient quality was significantly reduced. The M2 variant avoids this but  
 271 remains stochastic.
- 272 3. M3: In this approach, the first  $M$  rows of the Hadamard matrix (including the row  
 273 with all values equal to +1) are always selected for each iteration of the optimization.  
 274 This variant is therefore deterministic.

275 We finally note that the near-orthogonality and  $D$ -optimality of  $UE(s^2)$ -optimal de-  
 276 signs does not hold for the case  $N = 3(\text{mod } 4)$  where  $M > \frac{(N+5)}{2}$  (Jones and Majumdar,  
 277 2014). However, by choosing  $M$  properly, the design can be made  $D$ -optimal for this case  
 278 as well.

## 279 Numerical experiments

### 280 Analytical toy problem

281 The various sampling strategies and designs were first used for gradient estimation in a  
 282 simple toy problem for which exact gradients can be computed analytically. We used an  
 283 extended version of the well-known Rosenbrock benchmark function which is characterized  
 284 in 2D by a curved valley, with a minimum at coordinates (1, 1) located in one of the two  
 285 branches of the valley. In order to mimic the high dimensionality typically encountered  
 286 in subsurface reservoir problems, we use the extended Rosenbrock function (Dixon and  
 287 Mills, 1994). In addition to a large numbers of controls we want to investigate the impact  
 288 of uncertainty in the model properties. Therefore, uncertainty is introduced to mimic the  
 289 geological uncertainty following (Fonseca et al., 2015a),

$$J(u_1, \dots, u_N, c_1^j, c_2^j) = \sum_{i=1}^{N/2} -(\sin c_2^j)(1 - u_{2i-1})^2 - 100(c_1^j u_{2i} - u_{2i-1}^2)^2, \quad \text{for } j = 1, \dots, M, \quad (9)$$

290 where  $(c_1^j, c_2^j)$  with  $j = 1, \dots, 100$  are samples from  $\mathcal{N}(0, \mathbf{I}_2)$  representing  $M = 100$  model  
 291 realizations, and  $N$  is the number of controls which we set here to 320. The gradient of  
 292 Eq. (9) can be derived analytically for any set of controls.

293 The iterative objective function increase during optimization is commonly character-  
 294 ized by fast improvements during early iterations when objective function values are far  
 295 from the optimum (the objective function curve is steep), and very slow improvement  
 296 towards convergence (the objective function curve is nearly flat). We are interested in  
 297 determining the quality of gradient estimates during both stages of the optimization pro-  
 298 cess. Several trial optimization experiments were conducted with randomly distributed  
 299 initial controls from which intermediate solutions were assigned to one of two point sets  
 300 representing the two described stages. The quality of ensemble gradients was subsequently

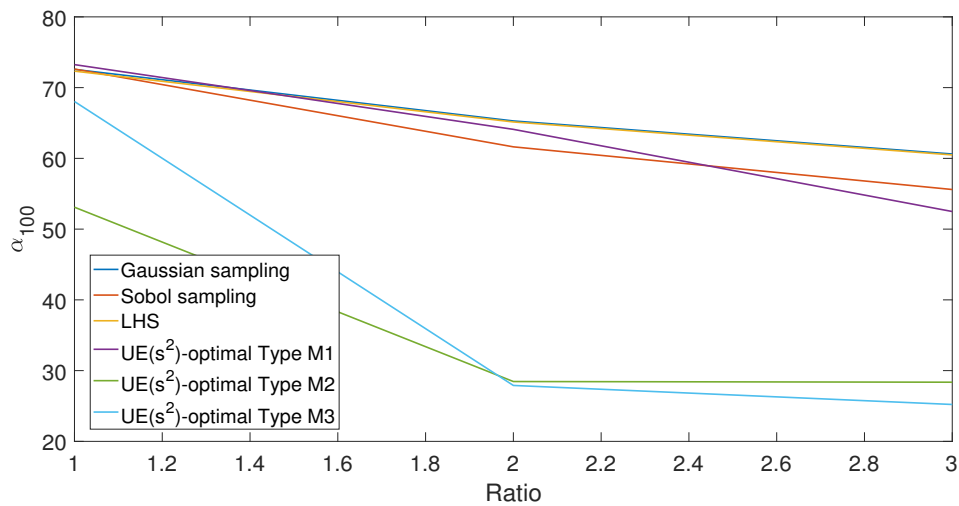


**Figure 2: Mean gradient direction error  $\alpha_{100}$  at points associated with large objective function improvements for  $\frac{M}{N_r}$  ratios 1, 2 and 3 and different sampling strategies using a standard deviation  $\sigma$  of 0.01. The true and estimated gradients represent the expected values over 100 different model realizations.**

301 determined at each point in the two sets. For sampling strategies involving random num-  
 302 bers the gradient computation was repeated 100 times, after which an average angle error  
 303 was computed by comparison with the analytical gradient direction. The standard devia-  
 304 tion of the control perturbation magnitude was set to 0.01 in all cases. The quality of the  
 305 estimated gradients, as quantified by the average angle error, is shown in Figs. 2 and 3.  
 306 The angle error is estimated for different ratios  $\frac{M}{N_r}$  where  $N_r$  is the number of model real-  
 307 izations. If the ratio equals 1, we use the same number of perturbations as there are model  
 308 realizations, while if the ratio equals for example 3, three different perturbed controls are  
 309 applied to each model realization. Figure 2 shows the average angle error  $\alpha_{100}$  for 3 ratios  
 310 and different sampling strategies for control points associated with the steep part of the  
 311 objective function curve while Figure 3 shows the average angle error for control points  
 312 associated with the near-flat part of the objective function curve.

313 During the initial iterations of the optimization, the Gaussian, Sobol, LHS and  
 314  $UE(s^2)$ -M1 sampling strategies provide a similar gradient quality for a ratio of 1:1 (Fig.  
 315 2). A slight difference is seen when the ratio is increased to 3 with  $UE(s^2)$ -M1 and Sobol  
 316 performing slightly better on average than the Gaussian and LHS strategies. For a 1:1  
 317 ratio,  $UE(s^2)$ -M2 and M3 provide the best gradient quality, with angle errors that are  
 318  $5^\circ$  to  $30^\circ$  lower than for the other strategies. Gradient direction errors are significantly  
 319 larger for the later stages of the optimization as seen in Fig. 3. Otherwise the results are  
 320 more or less consistent with those for the early stage except that the differences between  
 321  $UE(s^2)$ -optimal designs of type M2 and M3 and Gaussian, Sobol, LHS and  $UE(s^2)$  -  
 322 optimal design of type M1 are relatively smaller. In conclusion, for the high-dimensional  
 323 Rosenbrock function with uncertainty,  $UE(s^2)$ -optimal designs of type M2 and M3 pro-

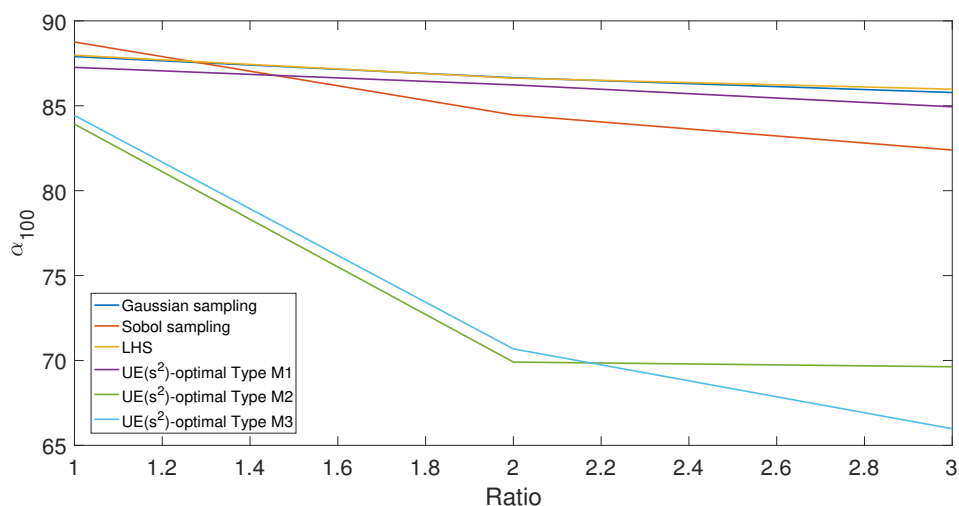


**Figure 3: Mean gradient direction error  $\alpha_{100}$  at points associated with small objective function improvements for  $\frac{M}{N_r}$  ratios 1, 2 and 3 and different sampling strategies using a standard deviation  $\sigma$  of 0.01. The true and estimated gradients represent the expected values over 100 different model realizations .**

324 vide significantly better gradients than the other sampling strategies, especially in the  
 325 early stages of the optimization process when solutions are far from the optimum.

326 Oil reservoir case

327 In this section we will investigate the impact of the different sampling strategies on an  
 328 optimization process for a small, but realistically complex, reservoir test case. The 3D  
 329 reservoir model used in this thesis is the 'Egg' benchmark model (Van Essen et al. (2009);  
 330 Jansen et al. (2013)). Figure 4 shows the permeability field of one model realization and  
 331 the position of eight injection wells (blue) and four production wells (red). The egg model  
 332 is a channelized reservoir model with seven vertical layers and a total of 18553 active cells.  
 333 The permeability values are not conditioned to values at the wells, and the porosity is  
 334 assumed to be constant. The producers are operated at constant bottom hole pressure,  
 335 while the injectors are rate-controlled between 10 and 79.5 m<sup>3</sup>/day. Production of the field  
 336 is simulated for a period of 3600 days which is discretized into 40 control time intervals  
 337 of 90 days. This results in a total of 40  $\times$  8 = 320 injection rate controls. The objective  
 338 function used in this work is the undiscounted Net Present Value (NPV), i.e. the sum of  
 339 revenues and costs induced over the production period. We use an oil price of 126 \$/m<sup>3</sup>  
 340 and costs of 19 \$/m<sup>3</sup> and 6 \$/m<sup>3</sup> for water production and injection respectively. The  
 341 fully implicit black oil simulator OPM Flow is used for the model simulations and the  
 342 objective function is computed based on the simulator output. We investigate both the  
 343 deterministic and robust optimization cases, where the model realizations are taken from  
 344 a set of 100 permeability realizations. Six of these realizations are shown in Fig. 5. More  
 345 details on the model can be found in (Jansen et al., 2013).

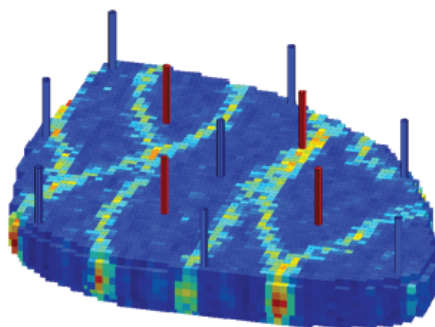


**Figure 4: Permeability field of an egg model of the reservoir with 8 injector wells (blue) and 4 producer wells (red)**

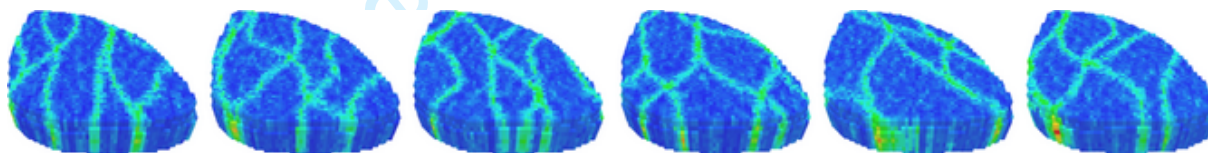


**Figure 5: Six randomly chosen model realizations, taken from (Jansen et al., 2013), characterizing the uncertainty in the permeability.**

### 346 Deterministic optimization

347 In deterministic optimization there is no uncertainty in the model, and therefore only a  
 348 single model realization is used in this section (i.e.  $N_r = 1$ ). All optimization experiments  
 349 are run for a fixed number of iterations (35) and use a steepest ascent update with a  
 350 normalized gradient (that is, the norm of the gradient vector is 1) and a fixed step size of  
 351 0.1. The convergence will thus be affected primarily by the quality of the gradient. The  
 352 initial control vector consists of equal values of 79.5 in units of  $\text{m}^3/\text{day}$  which corresponds  
 353 to the maximum injection rate.  $M = 100$  perturbation vectors are generated to estimate  
 354 the gradients by solving Eq. (4). Figures 6 and 7 show the objective function curves over  
 355 all iterations for different sampling strategies with the number of perturbation vectors  
 356  $M=100$  and  $M = 30$  respectively.

357 When  $M=100$  the curves for  $UE(s^2)$  designs of type M2 and M3 flatten after 14  
 358 iterations. The curve for Sobol sampling approaches the same final objective function  
 359 value at a slightly slower rate. These methods also produce high convergence rates and  
 360 final objective function values when the ensemble size is very small (30). From the results  
 361 of the Rosenbrock function it was observed that  $UE(s^2)$  designs of type M1 provides  
 362 inferior gradient quality compared to M2 and M3 at poor control points (steep section  
 363 of the objective function curve). This is also observed in Figs. 6 and Fig. 7. The curve  
 364 for M1 shows iteration intervals for which convergence is extremely slow, alternated by  
 365 intervals with steep increases in the objective function. Upon inspection it was discovered  
 366 that these intervals correspond to iterations in which the row of the Hadamard matrix  
 367 containing only +1 values was either not included (slow improvement) or was included

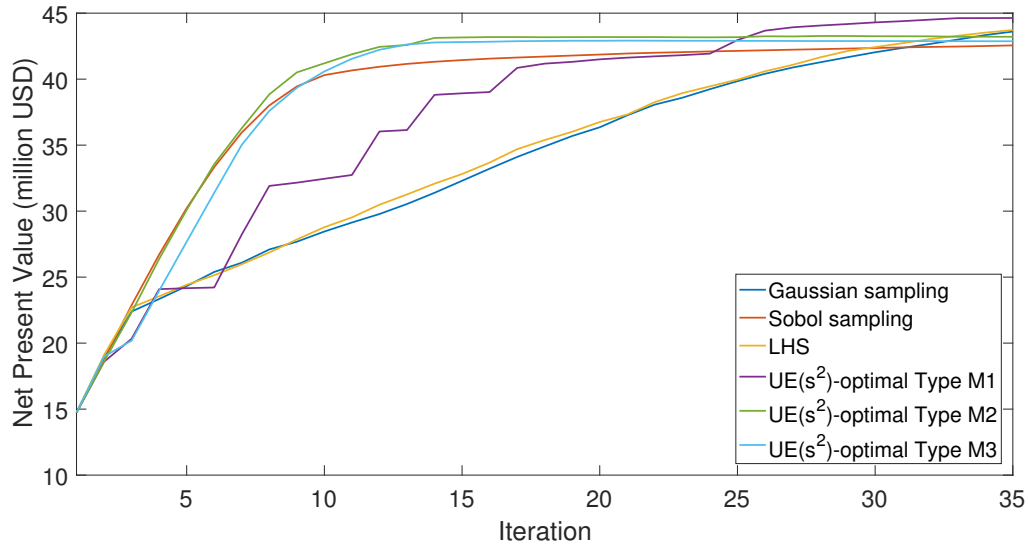


Figure 6: NPV as a function of optimization iteration using Eq. refeq:menopt with  $M = 100$  for different sampling strategies.

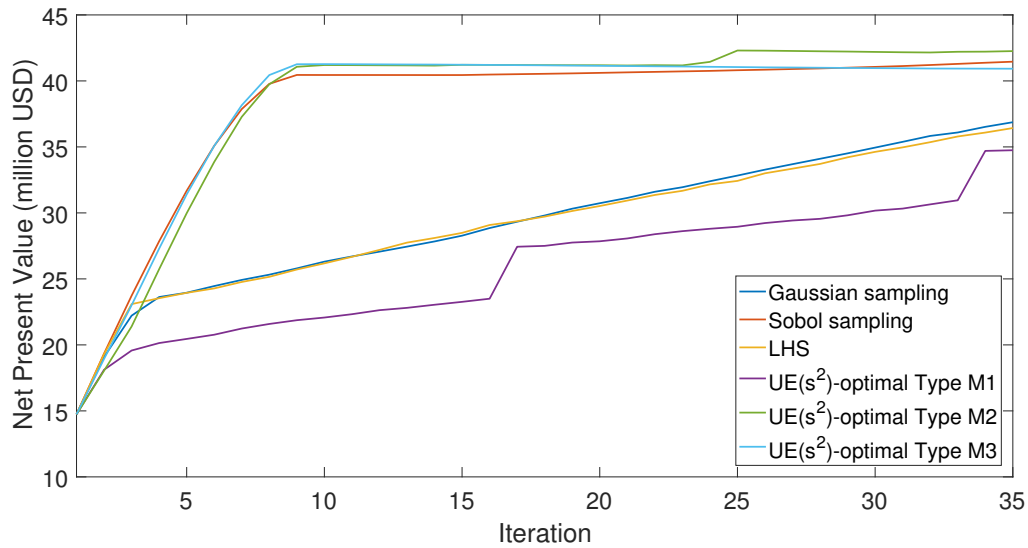
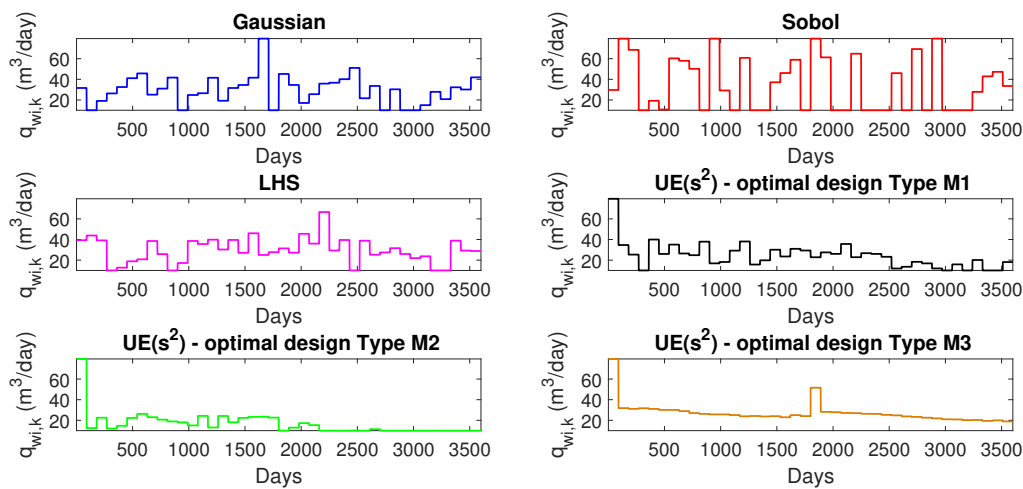


Figure 7: NPV as a function of optimization iteration using Eq. refeq:menopt with  $M = 100$  for different sampling strategies.



**Figure 8: Control strategy representing the injection rate of one of the injectors as a function of time at the final iteration (35) obtained with 6 different sampling strategies and  $M = 100$  and  $N_r = 1$ .**

368 (fast improvement). This behaviour actually motivated the creation of the new schemes  
 369 M2 and M3 in this paper. In general, both M2 and M3 perform slightly better than Sobol  
 370 sampling which tends to produce objective function curves that flatten a bit earlier. Since  
 371 the curves for Gaussian and LHS sampling have not yet flattened after 35 iterations, it is  
 372 not possible from these results to draw conclusions about the final objective function value  
 373 that can be reached. Given the high computational cost associated with simulating large  
 374 and complex reservoir models, it seems not unreasonable to consider the performance of  
 375 different methods for a limited number of iterations (or function evaluations). It appears  
 376 that LHS does not perform better than Gaussian sampling for the number of controls  
 377 considered in these experiments.

378 The optimal control strategies for one of the injectors obtained after 35 iterations  
 379 are shown in Fig. 8. The choice of sampling method clearly has a significant impact  
 380 on the character of the resulting control strategy. While Sobol sampling produces a  
 381 strategy with frequent and large changes in the injection rate, the  $UE(s^2)$  designs tend to  
 382 produce fairly smooth low-rate profiles. Highly-dynamic control strategies are generally  
 383 undesirable from an operational point of view. Regularization of the gradients is often  
 384 proposed as a means to produce smooth control profiles. One way to achieve this is  
 385 by imposing correlations over time between the control perturbations, i.e. between the  
 386 samples, through a smoothing step. The impact of this approach on the optimization  
 387 process for different sampling methods is illustrated in Fig. 9, where a correlation length  
 388 of 15 control intervals was applied (the total number of intervals is 40).

389 Correlation clearly benefits the convergence properties for all sampling methods except  
 390 Sobol sampling. Gaussian sampling, LHS and  $UE(s^2)$  designs all produce very similar  
 391 objective function profiles. Gaussian sampling and LHS produce the highest final objective



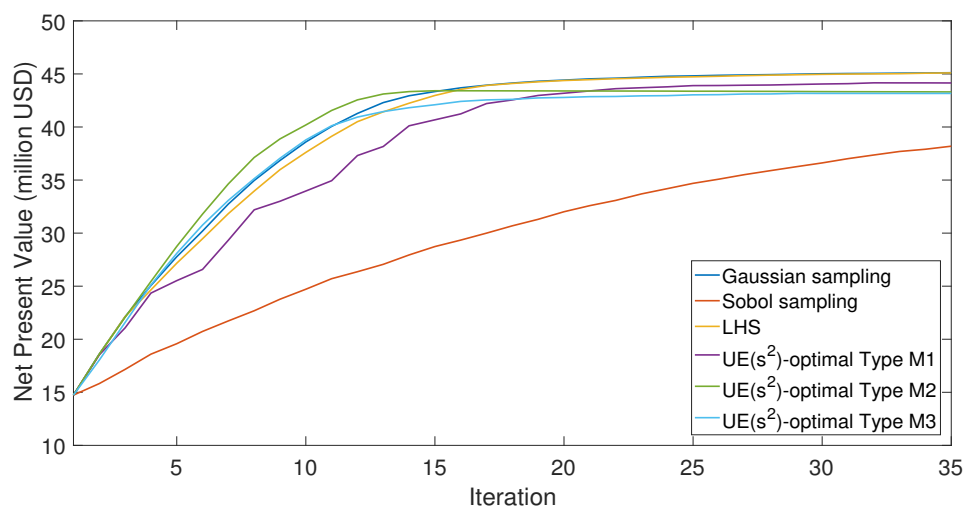


**Figure 9: NPV as a function of optimization iteration using Eq. refeq:menopt with  $M = 100$  and with smoothing of perturbations for different sampling strategies.**

392 function values, while the values obtained for  $UE(s^2)$  are nearly identical to those obtained  
 393 without induced correlation. The convergence rate for Sobol sampling on the other hand  
 394 has decreased notably. We conclude that this latter result must be related to the loss of  
 395 uniformity of Sobol distributions after smoothing.

### 396 Robust optimization

397 In this section the optimization is aimed at maximizing the expected NPV as evaluated  
 398 over 100 equiprobable realizations of the model with different permeability fields as il-  
 399 lustrated in Fig. 5. The gradient of the expected NPV is computed directly using the  
 400 formulation of Eq. (2) based on 100 control perturbation vectors that are paired on a  
 401 1:1 ratio basis to the model realizations. The perturbation standard deviation, random  
 402 seed, and initial controls are the same for all experiments and identical to those used in  
 403 the deterministic case. The optimization process is performed for a fixed number of 25  
 404 iterations (gradient evaluations). A lower value than used for the deterministic case was  
 405 chosen to limit the computational cost; in the robust case 100 simulations are required  
 406 to determine the objective function value for a proposed control update, whereas only 1  
 407 simulation is required in a deterministic setting. The results from experiments without  
 408 and with time correlations between controls are shown in Figs. 10 and 11 respectively.

409 The results indicate that the performance of the different sampling methods in the  
 410 robust optimization case is similar to that in the deterministic case. The main differences  
 411 are observed if time correlation is imposed on the samples. While in the deterministic  
 412 setting all methods except Sobol performed similarly, in the setting with model uncertainty  
 413  $UE(s^2)$  designs of type M2 clearly perform better than all other methods. Sobol sampling  
 414 still performs worse than all other methods. The use of time correlation leads to improved  
 415 objective function values when Gaussian, LHS and  $UE(s^2)$  sampling of type M1 is used,

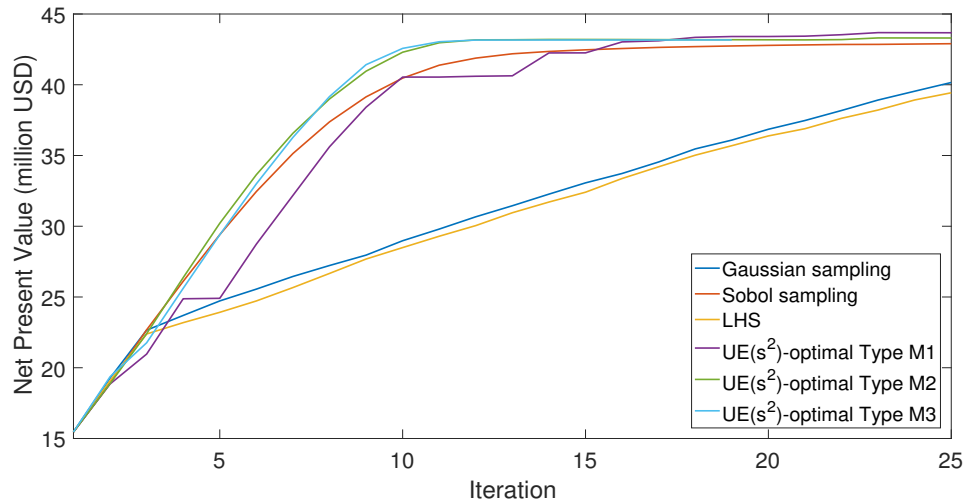


**Figure 10:** NPV as a function of optimization iteration using Eq. refeq:stosag with  $M = N_r = 100$  for different sampling strategies.

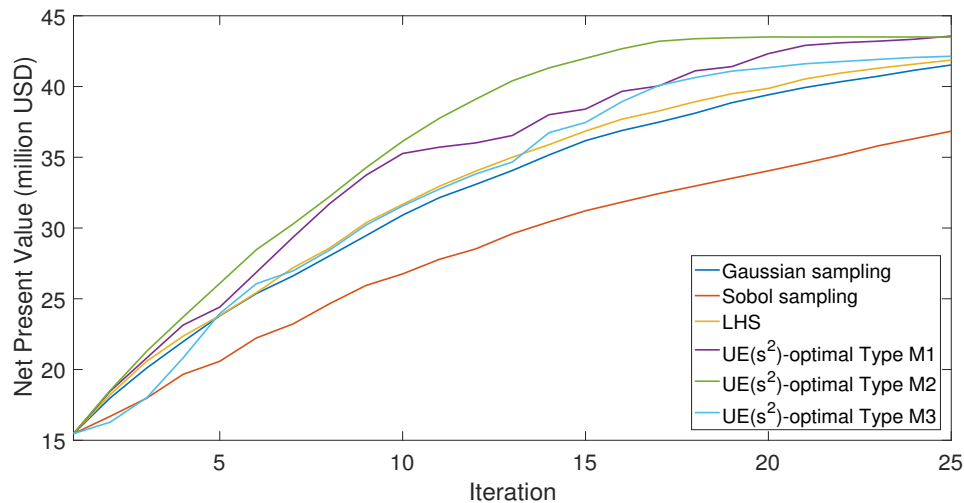


**Figure 11:** NPV as a function of optimization iteration using Eq. refeq:stosag with  $M = N_r = 100$  and with smoothing of perturbations for different sampling strategies.

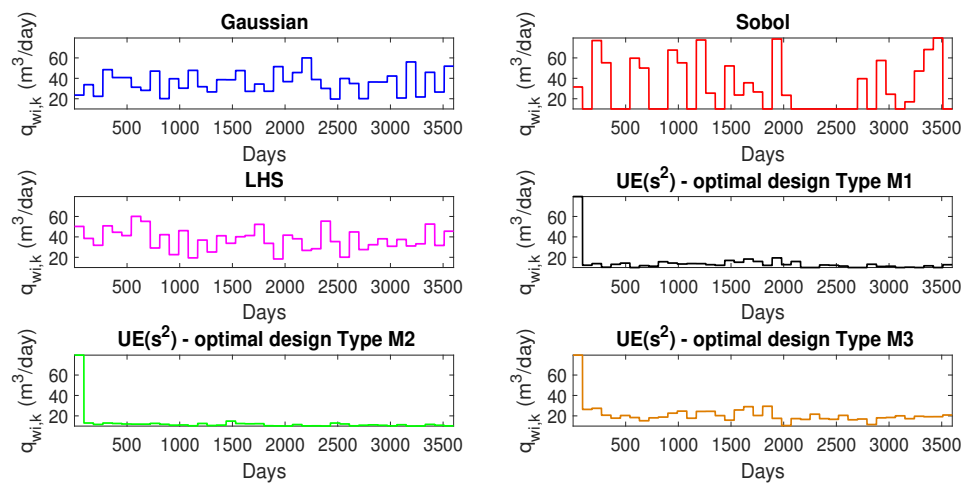


**Figure 12: Robust control strategy representing the injection rate of one of the injectors as a function of time at the final iteration (25) obtained with 6 different sampling strategies and  $M = N_r = 100$ .**

416 and to reduced objective function values when  $UE(s^2)$  sampling of type M3 or Sobol  
 417 sampling is used. The results for  $UE(s^2)$ -M2 are hardly affected.

418 The optimal control strategies obtained after 25 iterations are shown in Fig. 12 for  
 419 all sampling strategies. Similar behavior can be observed as in the deterministic case.  
 420 When using Sobol sampling, the water injection rate jumps between near-minimum and  
 421 near-maximum values. This is close to what is known as a bang-bang strategy, which  
 422 is an optimal strategy for certain linear problems and is characterized by solutions that  
 423 attain only the minimum and maximum allowable control values. The solutions obtained  
 424 with Gaussian sampling and LHS tend to vary around an intermediate average control  
 425 value, while the  $UE(s^2)$  solutions consistently suggest near-minimum injection rates. The  
 426 solutions for this well are characteristic for those of the other wells as well, with  $UE(s^2)$ -  
 427 based injection rates mostly in the range of 10 - 30 m<sup>3</sup>/day.

## 428 Discussion

429 The optimization experiments presented here were performed with the same constant  
 430 perturbation size. It has been observed in experiments with an different perturbation sizes  
 431 (Fonseca et al., 2015a) that smaller perturbations may be preferred during the later stages  
 432 of the optimization process. Ramaswamy (2017) compared the convergence with the  
 433 different sampling methods for three fixed perturbations sizes in optimization experiments  
 434 with the Egg reservoir model. The results suggest that the performance for  $UE(s^2)$  designs  
 435 of type M2 is much less sensitive to the perturbation size than that for Gaussian and Sobol  
 436 sampling or LHS designs.

437 Some of the considered sampling strategies, including Sobol sampling and  $UE(s^2)$

438 designs of type M3, are deterministic and therefore produce the same result each time.  
439 Strategies based on pseudo-random numbers (Gaussian, LHS), or on random selection of  
440 perturbations from a fixed set ( $UE(s^2)$  designs of type M1 and M2) may produce different  
441 results for different random number seeds. Ramaswamy (2017) investigated the sensitivity  
442 of the gradient quality and convergence with respect to the initial seed and found that this  
443 sensitivity is very large for  $UE(s^2)$  designs of type M1, but almost negligible for designs  
444 of type M2. This is another benefit of the  $UE(s^2)$ -type M2 designs proposed here.

## 445 Conclusions

446 The standard practice of using Gaussian sampling to generate random perturbations for  
447 use in approximate gradient estimation procedures is compared against various alternative  
448 sampling strategies. The alternative strategies include two space-filling designs, namely  
449 Sobol sampling and LHS, based on low-discrepancy concepts as achieved by quasi-Monte  
450 Carlo approaches and stratification respectively. A second class of methods is based on  
451 the  $E(s^2)$  near-orthogonality concept for supersaturated designs and D-optimal reduction  
452 of the generalized variance of the gradient estimate ( $E(s^2)$ -optimal designs). Two new  
453 variants of  $E(s^2)$ -optimal designs were proposed. The sampling strategies were applied to  
454 high-dimensional analytical test problem to evaluate their impact on the gradient quality.  
455 In a second example they were applied to an oil reservoir case with realistic complexity  
456 in terms of number of controls and uncertainty in parameter values to test their impact  
457 on optimization performance . The main conclusions can be summarized as follows.

- 458 • Sobol sampling and  $UE(s^2)$  designs outperform random sampling and stratified  
459 experimental designs in terms of gradient quality and convergence properties in all  
460 cases when no smoothing is performed on the samples prior to gradient estimation.
- 461 • When samples are smoothed over time the performance of Sobol sampling strongly  
462 deteriorates.
- 463 • The sampling strategy is found to have a significant impact on the character of  
464 the resulting control strategy. Sobol sampling tends to produce highly dynamic  
465 strategies, while  $UE(s^2)$  designs produce fairly smooth strategies, also when no  
466 smoothing is explicitly applied.
- 467 • The new  $UE(s^2)$  design referred to here as M2 was observed to outperform the  
468 optimal supersaturated design method previously suggested (M1), as well as a third  
469 variant (M3), in terms of performance of the optimization and in terms of sensitivity  
470 to the perturbation size and initial random seed.
- 471 •  $UE(s^2)$ -optimal supersaturated designs perform well in all situations that were in-  
472 vestigated for both deterministic and robust cases and are therefore recommended  
473 for gradient approximation schemes where the number of samples is less than the  
474 number of unknowns.

475 **References**

- 476 Booth, K. H. V. and Cox, D. R. (1962). Some systematic supersaturated designs. *Tech-*  
477 *nometrics*, 4:489–495.
- 478 Brouwer, D. R. and Jansen, J. D. (2004). Dynamic optimization of waterflooding with  
479 smart wells using optimal control theory. *SPE Journal*, 9(4):391–402.
- 480 Caffisch, R. E. (1998). Monte carlo and quasi-monte carlo methods. *Acta Numerica*,  
481 7:1–49.
- 482 Cavazzuti, M. (2013). *Optimization Methods : From Theory to Design Scientific and*  
483 *Technological Aspects in Mechanics*. Springer, ISBN: 978-3-642-31186-4.
- 484 Chen, Y. (2008). Efficient ensemble based reservoir management. *PhD Thesis, University*  
485 *of Oklahoma, USA*.
- 486 Custodio, A. and Vicente, L. (2007). Using sampling and simplex derivatives in pattern  
487 search methods. *SIAM Journal on Optimization*, 18(2):537–555.
- 488 de Aguiar, P. F., Bourguignon, B., Khots, M. S., Massart, D. L., and Phan-Than-  
489 Luu, R. (1995). D-optimal designs. *Chemometrics and Intelligent Laboratory Systems*,  
490 30(2):199–210.
- 491 Diego, G., Loyola, R., Pedergrana, M., and Garcia, S. G. (2016). Smart sampling and  
492 incremental function learning for very large high dimensional data. *Neural Networks*,  
493 78:75–87.
- 494 Dixon, L. C. W. and Mills, D. J. (1994). Effect of rounding errors on the variable metric  
495 method. *Journal of Optimization Theory and Applications*, 80(1):175–179.
- 496 Do, S. and Reynolds, A. (2013). Theoretical connections between optimization algorithms  
497 based on an approximate gradient. *Computational Geosciences*, 17(6):959–973.
- 498 Fonseca, R. M., Chen, B., Jansen, J. D., and Reynolds, A. (2016). A stochastic simplex  
499 approximate gradient (stosag) for optimization under uncertainty. *International Journal*  
500 *for Numerical Methods in Engineering*, 109(13):1756–1776.
- 501 Fonseca, R. M., Kahrobaei, S., Van Gastel, L. J. T., Leeuwenburgh, O., and Jansen, J. D.  
502 (2015a). Quantification of the impact of ensemble size on the quality of an ensemble  
503 gradient using principles of hypothesis testing. *Paper SPE 173236-MS presented at the*  
504 *SPE Reservoir Simulation Symposium, Houston, USA, 23-25 February*.
- 505 Fonseca, R. M., Leeuwenburgh, O., Van den Hof, P. M. J., and Jansen, J. D. (2015b).  
506 Improving the ensemble optimization method through covariance matrix adaptation  
507 (cma-enopt). *SPE Journal*, 20(1):155–168.

- 508 Fonseca, R. M., Stordal, A. S., Leeuwenburgh, O., den Hof, P. M. J. V., and Jansen,  
509 J. D. (2014). Robust ensemble-based multi-objective optimization. *Proceedings of the*  
510 *14th European Conference on the Mathematics of Oil Recovery (ECMOR XIV), 8-11*  
511 *September, Catania.*
- 512 Gilmour, S. G. (2006). Factor screening via supersaturated designs. In Dean, A. and Lewis,  
513 S., editors, *Screening : Methods for Experimentation in Industry, Drug Discovery and*  
514 *Genetics*, chapter 8, pages 169–190. Springer-Verlag New York.
- 515 Jansen, J. D., Bosgra, O. H., and Van den Hof, P. M. J. (2008). Model-based control of  
516 multiphase flow in subsurface oil reservoirs. *Journal of Process Control*, 18(9):846–855.
- 517 Jansen, J. D., Fonseca, R. M., Kahrobaei, S. S., Siraj, M. M., Van Essen, G. M., and  
518 Van den Hof, P. M. J. (2013). The egg model (research note). online, accessed July  
519 2017.
- 520 Jones, B. and Majumdar, D. (2014). Optimal supersaturated designs. *Journal of the*  
521 *American Statistical Association*, 109(508):1592–1600.
- 522 Kelly, C. T. (1999). Detection and remediation of stagnation in the nelder-mead algorithm  
523 using a sufficient decrease condition. *SIAM J. Optim.*, 10(1):43–55.
- 524 Lin, D. K. J. (1993). A new class of supersaturated designs. *Technometrics*, 35:28–31.
- 525 McKay, M., Beckman, R., and Conover, W. (1979). A comparison of three methods  
526 for selecting values of input variables in the analysis of output from a computer code.  
527 *Technometrics*, 42(1):55–61.
- 528 Morokoff, W. J. and Caflisch, R. E. (1995). Quasi-monte carlo integration. *Computational*  
529 *Physics*, 122(2):218–230.
- 530 Niederreiter, H. (1978). Quasi-monte carlo methods and pseudo-random numbers. *Bulletin*  
531 *of the American Mathematical Society*, 84(6):957–1041.
- 532 Niederreiter, H. (1988). Low-discrepancy and low-dispersion sequences. *Journal of Num-*  
533 *ber Theory*, 30:51–70.
- 534 Okano, H. and Koda, M. (2003). An optimization algorithm based on stochastic sensitivity  
535 analysis for noisy objective landscapes. *SPE Journal*, 79(2):245–252.
- 536 Owen, A. B. (1997). Monte carlo variance of scrambled net quadrature. *SIAM Journal*  
537 *of Numerical Analysis*, 34(5):1884–1910.
- 538 Owen, A. B. (2013). Monte carlo theory, methods and examples.
- 539 Paskov, S. H. and Traub, J. (1995). Faster evaluation of financial derivatives. *J. Portfolio*  
540 *Management*, 22:113–120.



- 541 Ramaswamy, K. R. (2017). Improved sampling for ensemble-based reservoir optimisation  
542 under uncertainty, msc. thesis. *Eindhoven University of Technology*.
- 543 Sarma, P. and Chen, W. (2014). Improved estimation of the stochastic gradient with  
544 quasi-monte carlo methods. In *Proc. 14th European Conference on the Mathematics of*  
545 *Oil Recovery (ECMOR XIV), Catania, Italy, 8-11 September*.
- 546 Sarma, P., Chen, W., Aziz, K., and Durlofsky, L. (2008). Production optimization with  
547 adjoint models under non-linear control-state path inequality constraints. *SPE Reser-*  
548 *voir Evaluation and Engineering*, pages 326–339.
- 549 Spall, J. (1992). Multivariate stochastic approximation using a simultaneous perturbation  
550 gradient approximation. *IEEE Transactions on Automatic Control*, 37(3):332–341.
- 551 Stordal, A. S., Szklarz, S. P., and Leeuwenburgh, O. (2016). A theoretical look at  
552 ensemble-based optimization in reservoir management. *Mathematical Geosciences*,  
553 48(4):399417.
- 554 Van den Hof, P. M. J., Jansen, J. D., Van Essen, G., and Bosgra, O. H. (2009). Model  
555 based control and optimization of large scale physical systems-challenges in reservoir en-  
556 gineering. *Chinese Control and Decision Conference, June 17-19, 2009, Guilin, China*.
- 557 Van Essen, G., Zandvliet, M., Van den Hof, P., Bosgra, O., and Jansen, J. D. (2009).  
558 Robust waterflooding optimization of multiple geological scenarios. *SPE Journal*,  
559 14(1):202–210.
- 560 Wu, C. F. J. (1993). Construction of supersaturated designs through partially aliased  
561 interactions. *Biometrika*, 80:661–669.